Software Resources for Remanence Estimation

Pratt, D.A.[1]

1. Tensor Research David.Pratt@tensor-research.com.au

ABSTRACT

The recovery of magnetic remanence information from magnetic survey data is covered extensively in research publications, but only a small proportion of the methods become widely available in commercial software applications. This paper explores some of the latest techniques that are available from software vendors that contribute value to the understanding of magnetic remanence estimation for mineral exploration. Modelling and inversion of magnetic remanence has been available for some time, but recovery of the magnetization direction and amplitude (resultant magnetization) is a relatively recent development. We examine the methods of direct estimation, parametric inversion and voxel inversion of resultant magnetization.

INTRODUCTION

There are many software tools and techniques used to assist in the interpretation of magnetic data where magnetic remanence may be present and there have been many advances in the last 10 years. The primary focus is on commercially supported products that are likely to see widespread use in the mineral exploration industry. Reference is made to academic research projects that may become available in future years. The review by Clark (2014) offers the most comprehensive coverage of current techniques for the recovery of remanent magnetization.

In this paper I emphasise geologically constrained parametric inversion using ModelVision (Pratt, 2013) which allows me to investigate soft or hard geological constraints. Our research results show how to recover the magnetization direction of the target and the importance of constraining the inversion process to achieve realistic results. I also illustrate how remote remanence estimation can be achieved in special circumstances once you have recovered the magnetization direction of the target. The limitations of these methods and the factors that contribute to estimation errors are reviewed as part of the discussion.

Remote remanence estimation (RRE) has potential in greenfields exploration to aid in the prioritization of a range of mineral commodities. Our research into different deposit styles and their associated magnetic minerals produced a set of diagnostic values for each style as a function of magnetic susceptibility and Koenigsberger ratio (Table 1). This requires the unique separation of the Koenigsberger ratio (Q) and magnetic susceptibility which can be done for cases suited to the RRE process.

The magnetic method is used as a fundamental mapping tool in most mineral exploration projects, so any magnetic remanence interpretation tool that can add value to the exploration objectives should be considered an integral part of the geophysicists toolkit.

Table 1. Diagnostic Value for Q and Magnetic Susceptibility combinations based on the range of Q and log range of susceptibility scaled to a diagnostic range of 1 to 5.

Deposit Style	Q	Susc	Diag
Diamond bearing kimberlite/lamproite pipes	2	3	5
Magmatic magnetite and banded iron formation (BIF) deposits	4	5	5
Massive iron oxide-copper-gold-uranium-rare-earth deposits (IOCG)	4	5	5
Massive magmatic ilmenite-haematite deposits	5	2	5
Polymetallic Cu-Zn-Au and Pb-Zn-Ag turbidite hosted deposits	3	4	5
Pyrrhotite skarn deposits	5	3	5
Archaean komatiite hosted nickel deposits	3	3	4
Magnetite skarn deposits	3	4	4
Porphyry copper-epithermal gold deposits	3	3	4
Mafic-ultramafic hosted (Alaskan Type) chromite/PGE deposits	1	4	3
Podiform intrusive deposits with ophiolitic affiliations	3	5	3
Massive sulphide deposits with BIF, amphibolite or basic igneous activity	2	3	2
Sedimentary (SEDEX) and related massive sulphide (Pb, Zn) deposits	2	1	2

TARGET RESOLUTION

As a precursor to the use of software to recover magnetic remanence, it is important to understand what resolution can be achieved and how this sets a limit on your expectations for detailed geological information definition.

In reality, we need to consider the geological model that is being applied in the exploration. In greenfields and brownfields exploration we usually work with magnetic data at a scale that makes it difficult to see local scale variations in the magnetic properties. That is, they look homogenous at distances equal to their lateral dimensions.

In target evaluation, the sensor measurements may be close enough to detect magnetic property variations within the target mass. This differentiation is very important and is often overlooked in conventional processing and inversion of magnetic data. Inferences are made from inversions that may not be detectable in practice. Forward modelling is the best way to test this potential limitation, particularly if you are planning to use voxel inversions.

Figure 1 shows the computed model responses for an east west line over a vertical series of magnetic formations, each 25 metres wide and exposed at the ground surface. Their magnetic susceptibilities alternate between 0.01 and 0.005 SI units. No magnetic remanence is used in this model. This comparison is important for understanding the limits of resolution of different surveys ranging from ground surveys at two metre sensor clearance to conventional fixed wing surveys at 80 metres clearance.

The total magnetic field is shown in red in Figure 1 and the vertical magnetic gradient in blue. The individual formations are clearly visible in the ground magnetic survey, but even at 25 metres clearance, the edges of individual formations have started to merge with adjacent formation and at 80 metres, appear to merge into a single formation.

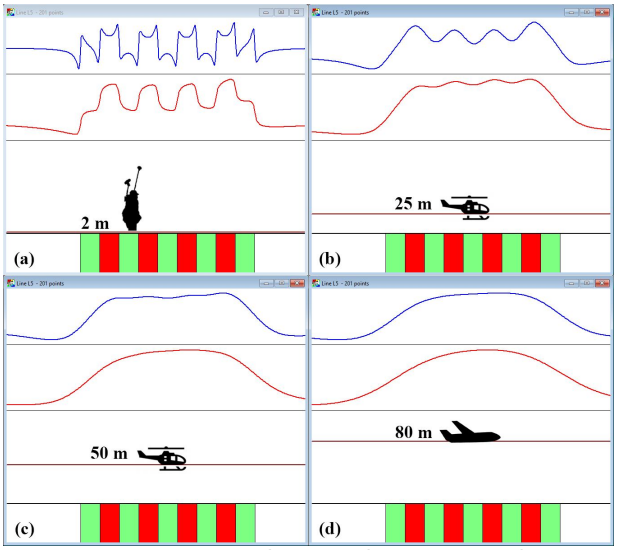

Figure 1. Resolution as a function of survey height for (a) 2m ground survey, (b) 25m helicopter survey, (c) 50m helicopter survey and (d) conventional aircraft survey at 80m clearance. The red curve is total field and the blue curve is vertical gradient. Each formation is 25m wide and starts at the ground surface.

These models are important for setting the scene as to what resolution we can realistically expect to extract from the inversion of magnetic surveys. This limitation can also work in our favour because at some scale, a magnetic unit looks like a homogenous unit despite the fact that internally, its properties can vary widely.

A useful rule of thumb says that "**the limit of horizontal resolution is approximately equal to the flying height**".

Next we need to consider the nature of magnetic property variations within the target formation that we wish to interpret. If we consider a basaltic pipe or dyke, we might expect its property in aggregate to be consistent over relatively large distances. On the other hand, an intrusion that is both magnetic and subject to hydrothermal alteration is likely to have a magnetization that varies continuously as a function of the alteration. In aggregate, it may appear homogenous at 80 metres, but a ground magnetic survey may discern these variations.

These considerations determine both the type of software tool that you need to use to obtain physical property information and the maximum ground clearance requirements for planned magnetic surveys.

MAGNETIZATION ESTIMATION

There are three basic approaches adopted by the exploration industry for the estimation of rock magnetization;

- Direct estimation
- Parametric inversion
- Voxel inversion.

Figure 2 illustrates the relationship between the induced field vector (red), remanent magnetization vector (black) and resultant magnetization vector (blue). They must all lie on the one plane and if we know any two of the vectors, we can determine the third. If we know the direction of the remanent magnetization from polar wander data, then we can calculate the magnetic remanence amplitude by using the induced field vector direction and resultant magnetization vector direction and amplitude.

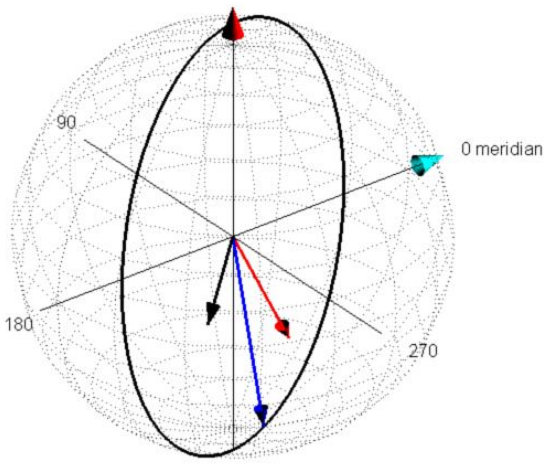

Figure 2. Illustration of the great circle plane containing the induced (red), remanent (black) and resultant (blue) magnetic field vectors.

Direct Estimation

Direct estimation methods such as the Schmidt and Clark (1998) method or Fedi et. al. (1994) focus on the analysis of isolated magnetic anomalies and require no model or inversion procedure. Schmidt and Clark (1998) implemented the Helbig (1963) magnetic moment method using FFT transformation of the total magnetic field grid to individual field components (Bx, By, Bz).

Encom Technology implemented this procedure in the products known as ModelVision and QuickMag. Tensor Research

continues to develop this capability within ModelVision. Figure 3 illustrate the application of the magnetic moment method to the Black Hill Norite anomaly C as defined by Foss and McKenzie (2012). The centre of magnetization is required for accurate computation of the magnetization vector so a seed model is used to estimate the centre. The initial position can be estimated from the peak of the normalized source strength anomaly or in this case its most central location.

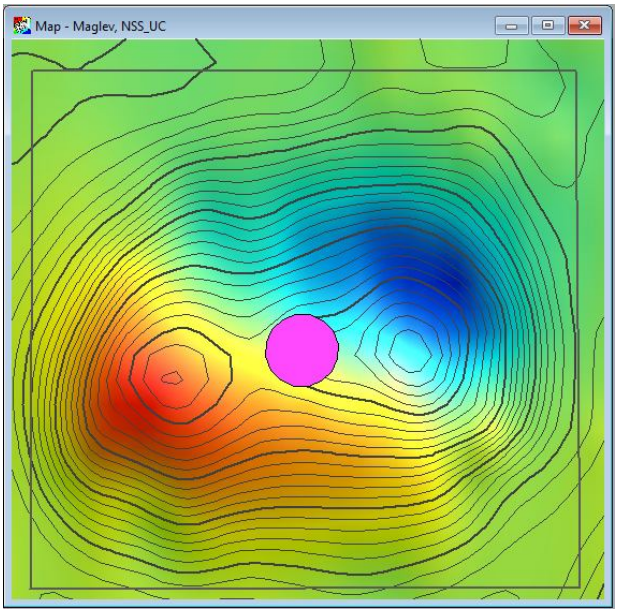

Figure 3. Black Hill Norite Anomaly C, without any filtering overlain by contours of the upward continued normalized source strength (NSS). The contours help to position the target centre of magnetization.

The magnetization vectors for the anomaly are shown in a dialog where the user can experiment with different data boundaries, body locations, susceptibilities and regional adjustments (Figure 4). The user can experiment with the body style and size to produce realistic volume estimates. The apparent resultant rotation angle (ARRA) between the local geomagnetic field and the resultant magnetization vector is an important parameter for the anomaly.

The regional magnetic field must be removed prior to the analysis, although and adjustment can be applied for a residual correction within the interpreter's dialog (Figure 4).

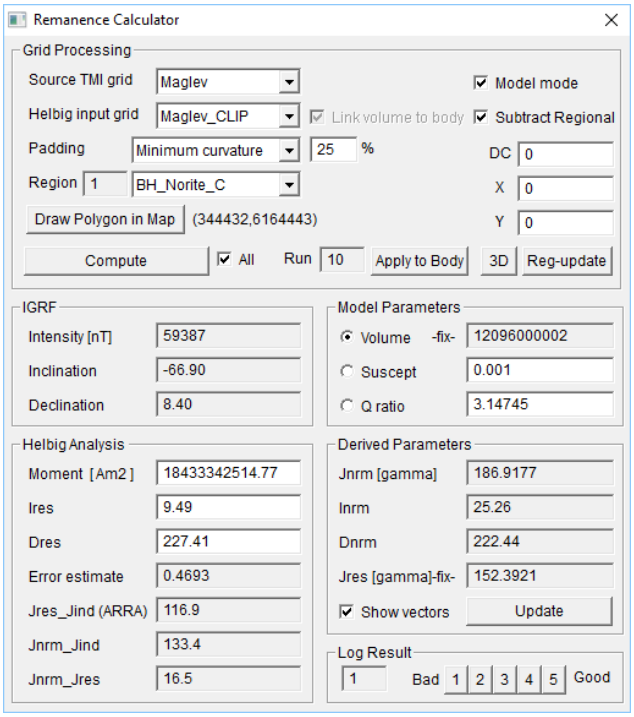

Figure 4 Process dialog with input and derived magnetization parameters from the Helbig analysis.

The relationships between the induced, remanent and resultant magnetization vectors are visualized in a small 3D viewer (Figure 5).

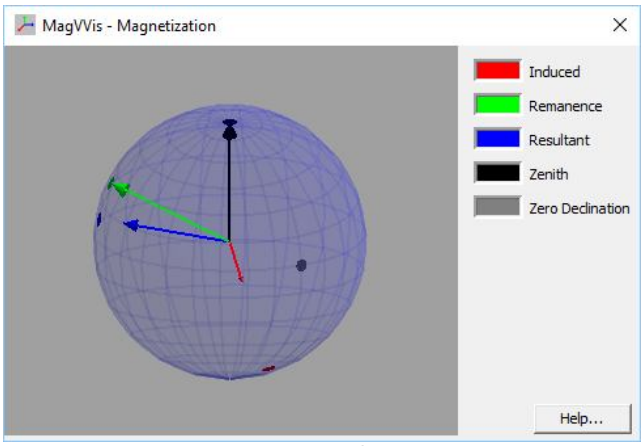

Figure 5 Interactive visualisation of the resultant magnetization vector (blue) along with the induced (red) and remanent field (green) vectors.

Cordani (2013) demonstrated the application of the Fedi et. al. (1994) method on the Black Hill Norite total magnetic intensity anomaly. This procedure known as the max-min method applies an iterative reduction to pole to find a magnetization inclination and declination that produces the smallest negative RTP anomaly.

The magnetization direction recovered from this method produced an inclination of 7.5 degrees and declination of 234

degrees. This is very close to the inversion results of 9 and 234 degrees respectively (Pratt et. al. 2012). The major limitations of this method relate to adequate removal of the regional magnetic field and interference overlap from nearby magnetic anomalies. Importantly, you can make a visual assessment of the final anomaly and make a value judgment of the quality of the final RTP transformation as shown in Figure 6.

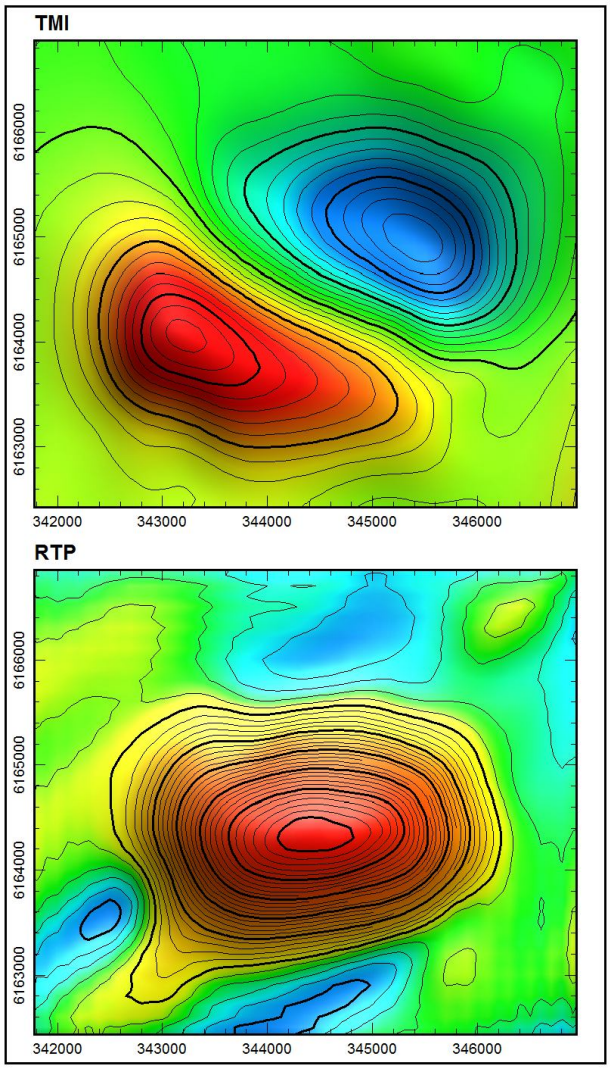

Figure 6. Example of the max-min method (bottom) applied to an upward continued version of the Black Hill Norite Anomaly C (top).

It is important to note that the magnetic moment and min-max methods recover the vector direction of the magnetization, but not the amplitude. The Helbig method recovers the magnetic moment and if you can estimate the volume of the target, then you can also recover the magnetization amplitude.

Parametric Inversion

For a long period of time, geophysicists believed that you could not recover magnetization direction through inversion of a magnetic model. This assumption was based on many textbook examples of the ambiguity between the dip and magnetization direction for dipping dyke-like bodies.

For long, straight dyke-like bodies, this limitation is true. But as demonstrated with the magnetic moment and min-max methods, it is possible to recover the magnetization direction of a magnetic source with a compact 3D shape where the data surrounds the full extent of the associated magnetic anomaly.

Given the success with these direct methods of estimation, we added resultant magnetization parametric vector inversion to ModelVision to complement the magnetic remanence vector inversion. In the remanence inversion case, you must provide either a magnetic susceptibility or Koenigsberger ratio to derive the remanent magnetization direction. On the other hand, the resultant magnetization vector inversion gives you the critical target parameter.

Pratt et. al. 2012, 2013, 2014, did extensive tests on a range of geological body shapes to establish the validity of inverting for magnetization direction and amplitude. Table 2 shows the results of trial inversions for tabular and elliptic shaped models against a range of tabular body targets with varying spatial parameters and Q values. The table shows the average errors in recovering dip, azimuth, magnetization inclinations and declinations. When using the elliptic pipe for a target the errors increased as the dip of the target became very shallow, otherwise for steep dips the errors were relatively small.

Table 2 Errors for model parameters and B_{res}

Parameter recovered by inversion	Tabular Av. Error (14 models)	Elliptic Pipe Av. Error (7 models)
Dip	0.51°	2.49°
Azimuth	0.13°	0.91°
Depth (m)	0.82	9.43
Resultant inclination	0.29°	4.27°
Resultant declination	0.46°	6.65°

Figure 7 shows a series of remanently magnetized polygonal target shapes. Both tabular body and elliptic pipe shapes were used as the inversion models to see what impact a poor shape match had on magnetization direction determination. The results of these tests are summarized in Table 3.

Importantly, the magnetization inclination and declination errors are less than 1 degree, indicating that the shape is not important to the recovery of magnetization directions, provide the magnetic source has a compact 3D shape.

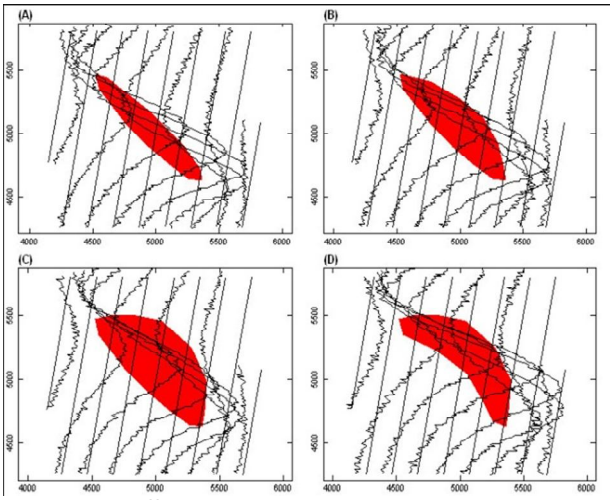

Figure 7. Different compact model shapes 200m below the sensor with 5% RMS random noise added to the computed total magnetic intensity. Tabular and elliptic shaped models were used in the inversions to recover the resultant magnetization vectors.

Table 3 Errors for model parameters and B_{res}

Parameter recovered by inversion	Tabular Av. Error (4 models)	Elliptic Pipe Av. Error (4 models)
Dip	2.38°	2.70°
Azimuth	0.93°	0.98°
Depth (m)	10.68	10.43
Resultant inclination	0.87°	0.80°
Resultant declination	0.46°	0.38°

From these experiments, we established that it was possible to reproduce the success of the magnetic moment and min-max methods for recovering the resultant magnetization vectors of compact magnetic sources without having to be precise with the model geometry. More importantly, we established that inversion could recover the body dip as well as the resultant magnetization vector.

Our research demonstrated that all methods are very sensitive to the impact of nearby sources and broader regional fields. If you do not model these correctly, then the magnetization direction will be in error. As a rough guide, a 1 degree error in the tilt of the background field will result in a 1 degree error in the magnetization direction.

We applied the inversion method to the total magnetic intensity data over the Black Hill Norite (Anomaly C) using the original line data immediately over the magnetic anomaly. A stacked profile map comparison of the magnetic field data with the inverted response is shown in Figure 8. The purple curves show the extent of the data used for inversion. Short wavelength anomalies superimposed on the original data are associated with younger, normally magnetized intrusion that cut through the norite. While these interfering features add to the noise, their wavelengths are sufficiently short that they have only a minor impact on the inversion results. The regional was also removed as part of the inversion.

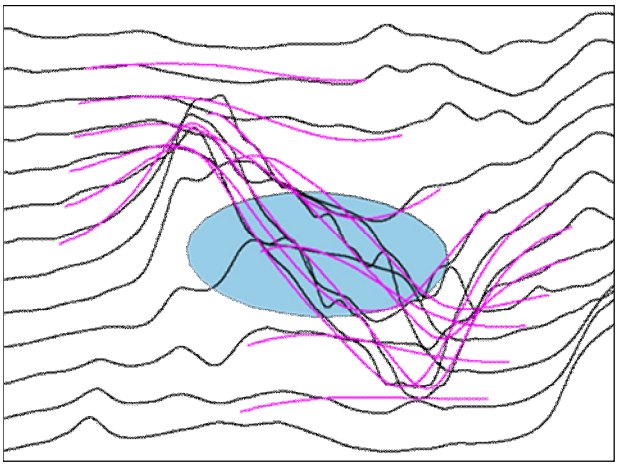

Figure 8. Balck Hill Norite Anomaly C stacked profile map of the measured total magnetic intensity (black) and the inverted model response (purple) for an elliptic pipe.

Table 4 shows the results of the inversion in row 5 compared with inversion (Res inv) and magnetic moment (MM 1, MM 2) results from Foss & McKenzie (2006, 2011) and Tensor Research (MM 1). The inversion results are very close with the inclination and declination values within 1 and 2 degrees respectively. The variation across the magnetic moment methods is larger than for the two inversions, but this is to be expected as there is less control of the regional, background estimation and centre of magnetization location.

Table 4 - Black Hill Norite Magnetization

Source	Method	Declin.	Inclin.
Foss & McKenzie, 2006	Res inv	232°	8°
Foss & McKenzie, 2006	MM 1	233°	12°
Foss & McKenzie, 2006	MM 2	223°	6°
Tensor Research study	**MM 1**	**227°**	**9°**
Tensor Research study	Res inv	**234°**	**9°**

While I am not aware of any other parametric magnetic inversion packages that allows direct inversion for resultant magnetization vector, an equivalent result can be achieved with remanent magnetization vector inversion by fixing the magnetic susceptibility at a very low value such as 0.000001 SI. The remanent vector is then equivalent to the resultant magnetization vector.

Voxel Inversion

The most popular voxel inversion software with support for magnetization inversion as a commercial solution include Voxi from Geosoft (MacLeod, 2013), and VPmg from Mira Geoscience (Faullagar and Pears, 2015). Each of these tools has provision for entering physical property constraints, but this increases the complexity of the task and in practice, many inversions are run without the benefit of basic geological

constraints. We note that unless a voxel or parametric model is geologically constrained it should be considered as a 3D equivalent source solution.

Geosoft's Voxi software is in widespread use and supports direct inversion for magnetization vector inversion as an alternative to magnetic property inversion. At the ASEG 2013 forum, MacLeod (2013) presented preliminary results for the Black Hill Norite Anomaly C (Figure 9). These results show that the vector directions are similar to those from the compact source modelling by Pratt et. al. (2012, 2014) and magnetic moment methods by Foss and McKenzie (2006) near the centre of the intrusion.

The larger remanent magnetic anomalies to the south-east show that the magnetization splits into separate regions within the intrusion. While this is a valid unconstrained equivalent source solution, we would expect the norite to have broadly the same magnetization across each intrusion.

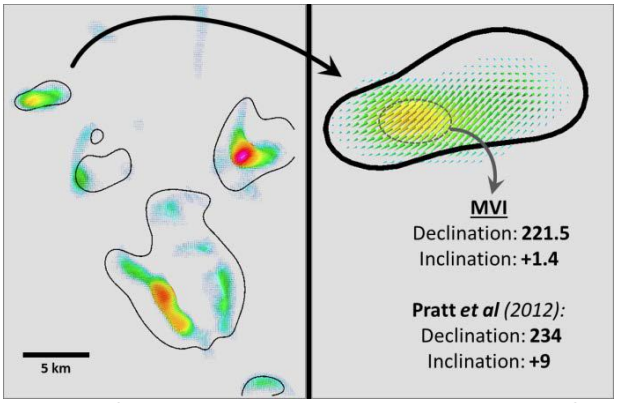

Figure 9. from MacLeod (2013) showing the results of the voxel inversion magnetization. Anomaly C is enlarged in the right hand section of the figure.

Voxi does provide a capability to include geological constraints for each target by modelling the target boundaries and with the application of constraints, we would expect the magnetization directions and amplitude to show less variation across each intrusion. However, the use of constraints in voxel modelling requires a lot more interpreter input and may not be justified when studying large areas.

By contrast, the parametric inversion is always constrained for shape and magnetization direction. For focus areas, it can be much faster to extract reliable magnetization vector information.

Research at the Colorado School of Mines (Li et. al., 2015) sponsored by the Magnetics Research Consortium and the University of British Columbia, Geophysical Inversion Facility (Lelievre and Oldenburg, 2009) sponsored by the GIFtools Consortium also addresses the requirement for direct magnetization inversion. At this time, the software is only available to project sponsors.

THOMSON OROGEN - CASE HISTORY

Our first systematic parametric inversion study using ModelVision focused on the simple shapes of the numerous magnetic pipes that are found in the southern Thomson Orogen in NSW, Australia (Figure 10).

The original flight line data for each anomaly was isolated, the background regional magnetic field modelled and an elliptic pipe shaped intrusion model response inverted against the data subset. A total of 100 magnetic anomalies were analysed and the results compiled across the region. A wizard was developed to prepare the flight line data for immediate inversion, with each target now taking around 3 minutes. Most inversions had a repeatability of better than 3 degrees, but the probable error in the bulk magnetization vector direction is likely to be higher and probably in the range 5 to 10 degrees depending upon the quality of the regional removal and interference from nearby magnetic anomalies.

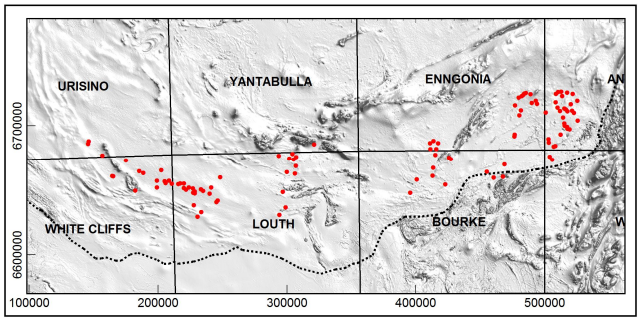

Figure 10. Locality map of the study area showing the 1:250,000 scale map sheet boundaries, targeted intrusive pipes (red) and southern Thomson Orogen boundary (dashed) over a shaded image of the reduced to pole magnetic grid.

A quality estimator (QE) was assigned to each inversion with values from 1 to 5, with 1 being the best quality and 5 the worst. The values are assigned based on an assessment of detrimental factors such as low anomaly amplitude, inversion RMS, small ARRA values, regional complexity and interference from nearby magnetic sources.

A cross-plot of the resultant inclinations and declinations is shown in Figure 11, where the size of the symbol has been modulated by the ARRA value (apparent resultant rotation angle) and the colour denotes the interpreter's quality estimation. Symbols in the upper half of the figure indicate a reversed magnetization direction.

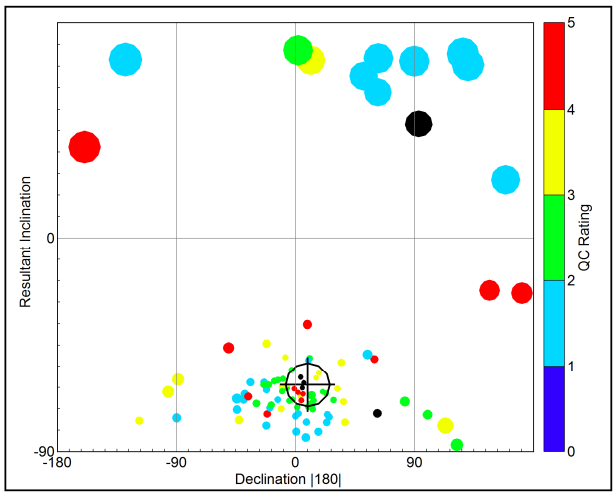

Figure 11. A cross-plot of the resultant magnetization vector direction as a function of inclination and declination and colour coded by the QC rating from the interpretation stage. The size of the symbol is based upon the total departure angle (ARRA) of the remanent vector from the induced field vector direction (IGRF black circle and + symbol).

The points closest to the field direction (small symbols) with magnetizations that are slightly steeper than the geomagnetic field and rotated in either clockwise or anticlockwise directions. There appears to be a separate population of larger rotations (intermediate size symbols) showing a broad range of magnetization directions. The scatter of these directions is much greater than expected for the expected precision of the method. The scatter could be related to continental drift due to a wide range of ages for the intrusions and secular variation in the magnetic field. Normally we would expect the secular scatter to be distributed randomly about the pole at the time of emplacement of the intrusion.

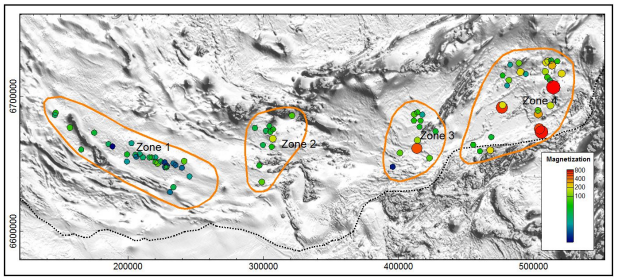

Figure 12. The distribution of resultant magnetization vector amplitudes modulated by symbol size and colour. A logarithmic scale is used for the colour axis. The intrusions are subdivided into four zones based only on their spatial concentrations.

Figure 13 shows the distribution of the apparent resultant rotation angle (ARRA) derived from the inversions where the symbol size and colour are modulated by the ARRA value. There was some expectation that the ARRA values would group in distinct geological zones and thus provide diagnostic geological information that could help differentiate intrusions.

The ARRA distribution appears to be similar in each of the four zones identified during the interpretation (Figure 12) and thus does not provide any useful geological discrimination in this particular study. This should not be taken as a general conclusion as we would expect some grouping to occur in other geological provences.

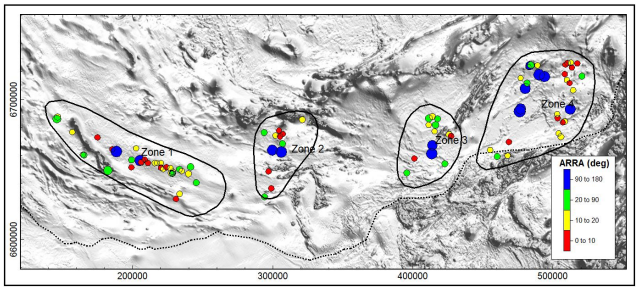

Figure 13. The distribution of the apparent resultant rotation angle (ARRA) modulated by symbol size and colour. Blue circles represent reversely magnetized pipes while red, yellow and green are normally magnetized.

RRE - REMOTE REMANENCE ESTIMATION

If you know from independent paleomagnetic information the remanent magnetization direction for the probable age of your intrusion, then you can calculate the remanent magnetization, Koenigsberger ratio (Q) and magnetic susceptibility. This method does not require a rock sample measurement from the target, just an estimate for the paleomagnetic direction.

The amplitude of the induced magnetization vector is unknown, but you do know the amplitude of the resultant magnetization vector from the inversion. The induced field vector, resultant magnetization vector and remanent magnetic vector all lie on the same plane and from this geometric relationship you can determine the amplitude of the induced magnetic field and remanent magnetic field. This allows you to determine a corrected magnetic susceptibility and a Koenigsberger ratio (Q).

Cordani and Shuwkosky (2009) demonstrated that you can resolve Q if you know the resultant magnetization direction recovered from the min-max method, but did not know it's amplitude. In this case, you cannot recover the true magnetic susceptibility or remanent magnetization amplitude.

We used polar wander data for Australia to determine the most likely pole position using interpolation between measured palaeopoles and then computed a corrected magnetic susceptibility and Q value for each intrusive pipe (Figures 14 and 15). The magnetic susceptibility distribution suggests that Zones 1, 2 and 3 have similar ranges., while Zone 4 has a much higher range of magnetic susceptibilities.

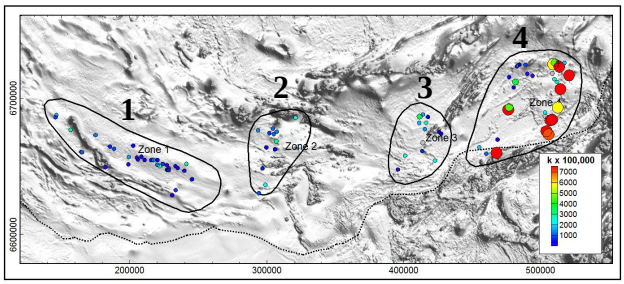

Figure 14. The distribution of magnetic susceptibility corrected for remanence. The magnetic susceptibility (SI x 10^{-5}) is shown as symbols modulated by colour and size using a histogram stretch.

The distribution of Q values in Figure 15 does not show any distinct differentiation between the four zones.

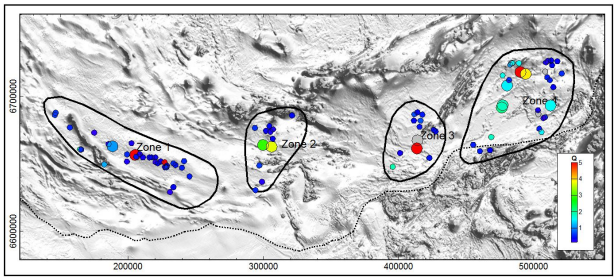

Figure 15. The distribution of the Koenigsberger ratio (Q) after estimation of the intrusion age. The large circles are reversely magnetized. The grey circle symbols have a null Q value assigned where QC> 5.

Figure 16 shows the distribution of intrusion ages based on finding the most appropriate paleopole direction.

It is important to note the ambiguity in selecting ages from the polar wander curves. In Zones 1, 2 and 3, there was often a choice between a Triassic age solution and one of Carboniferous age, but in other cases there was only one solution and that was generally of Carboniferous age. Late Carboniferous, Permian and Triassic are all difficult to separate, but if remanence vectors have reverse polarity then that would lend some evidence for the Late Carboniferous-Permian Superchron (P. W. Schmidt, 2013, pers. comm.). As a result, the ambiguous solutions were reclassified to Carboniferous or Late Devonian. No geological information was available to help with this classification, but this blind study was designed to test the merits of the method for age dating and further deductions that could be applied to the geological evolution of the region. The four green solutions in Zones 1 and 2 correspond to the Triassic and there was generally the option of a younger Cretaceous solution available.

Remote remanence estimation must still be regarded as an experimental method as there is no independent field verification of the technique over a wide range of geological ages.

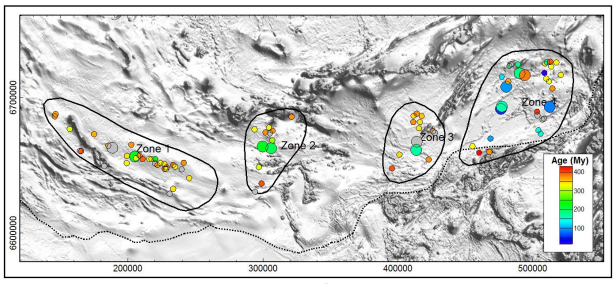

Figure 16. The distribution of intrusion ages modulated by symbol colour but including only higher quality solutions for QC ratings 1 to 3. Large symbols indicate that the anomaly is reversely magnetised. Where the QC class is higher than 3, it is shown as a grey circle. Symbols from yellow to red cover the late Devonian and Carboniferous periods, while light blue (cyan) to light green symbols indicate the Jurassic period. There are four green symbols that would correspond approximately with the Triassic.

CONCULSIONS

While there are many publications on the modelling and inversion of magnetic remanence and specifically magnetization, the number of commercially available tools is relatively small. The principal categories are based on direct, non-model based estimation, parametric inversion and voxel based inversion.

Direct estimation techniques such as the min-max method and ModelVision magnetic moment technique are convenient because they can be applied rapidly to a compact source anomaly. They are less precise than parametric inversions because there is less control over the estimation of the regional magnetic field and interference from adjacent magnetic anomalies.

Parametric inversion as used in ModelVision provides a geologically constrained approach to the estimation of the bulk magnetization of a compact magnetic source with full control over modelling of interfering anomalies and regional backgrounds. It can also be used to model complex environments with a mixture of induced and remanent magnetic formations. Isolation of the remanently magnetized compact source target is essential for the accurate estimation of the magnetization vector. Parametric modelling benefits from building geological constraints as a natural part of the process and focusing on quality results from individual anomalies or anomaly complexes.

There are two approaches available for voxel based methods where the VPmg approach is essentially a hybrid between pure parametric inversion and the pure property cell based inversions by allowing some variation in the cell vertical thickness. This has the advantage of reducing the number of cells required for an inversion compared with a pure property inversion. The Voxi approach is a pure property inversion, but it has the option of being constrained by a related geological model. The benefit of voxel model inversion is the ability to produce models for large survey areas. Unless the constraint model is included, the solution is an equivalent source model that lacks the property estimation precision achieved by parametric inversion for specific magnetic anomaly sources. Building a constraint model for a

large area is time consuming and is often applied to mine scale targets, but less so to greenfields exploration.

In this paper, I have discussed a range of software solutions for magnetic remanence studies in exploration using magnetic field data. The review by Clark (2014) provides an excellent summary of all possible methods for determining remanent and total magnetization.

ACKNOWLEDGEMENTS

The author would like to acknowledge Clive Foss for his enthusiastic encouragement to continue our research into methods for recovering remanent magnetization from magnetic data and his review of this publication. Also, much of the underlying research and development work has been undertaken by my colleagues K. (Blair) McKenzie and Tony White.

Mira Geoscience provided information on VPmg and references to work by Peter Fullagar and Glenn Pears. Mira Geoscience now develops and supports VPmg.

ModelVision is developed and supported by Tensor Research.

REFERENCES

Clark, D.A., 2014, Methods for determining remanent and total magnetisations of magnetic sources – a review: Exploration Geophysics, **45**, 271-304.

Cordani, R., and Shukowsky, W., 2009, Virtual Pole from Magnetic Anomaly (VPMA): A procedure to estimate the age of a rock from its magnetic anomaly only: Journal of Applied *Geophysics*, **69**, 96-102.

Cordani, R. 2013, Virtual Pole fromMagnetic Anomalies (VPMA) technique applied to Australian anomalies, in P.W. Schmidt, D.A. Pratt, C.A. Foss, eds., The Application of Remanent Magnetisation and Self- Demagnetisation Estimation to Mineral Exploration. Extended Abstracts, from the 2013 ASEG-PESA Forum, 48-54.

Fedi, M., Florio, G., and Rapolla,A., 1994, A method to estimate the total manetization direction from a distortion analysis of magnetic anomalies: *Geophysical Prospecting*, **42**, 261-274.

Foss, C. and McKenzie, B., 2006, Inversion of anomalies due to remanent magnetisation: an example from the Black Hill Norite of South Australia: Extended Abstracts, AESC2006, Melbourne Australia, 9p.

Foss, C. and McKenzie, B., 2011, Inversion of anomalies due to remanent magnetisation: an example from the Black Hill Norite of South Australia: Australian Journal of Earth Sciences **58**, 391-405.

Fullagar, P.K. and Pears, G.A., 2015, Remanent magnetization inversion: Extended Abstracts ASEG-PESA 2015, - Perth Australia, 4p.

Helbig, K.,1963, Some integrals of magnetic anomalies and their relationto the parameters of the disturbing body: Zeitschrift fur Geophysik, 29, 83-96.

Lelievre, P.G. and Oldenburg, D.W., 2009, A 3D total magnetization inversion applicable when significant, complicated remanence is present: Geophysics, **74**, L21-L30.

Li, Y. and Jiajia Sun, 2015, Towards geology differentiation using magnetization inversions: Extended Abstracts, GEM Chengdu 2015: International Workshop on Gravity, Electrical & Magnetic Methods and Their Applications Chengdu, China. April 19-22, 350-353.

MacLeod, I.N. and Ellis, R.G. 2013, Magnetic Vector Inversion, a simple approach to the challenge of varying direction of rock magnetization, in P.W. Schmidt, D.A. Pratt, C.A. Foss, eds., The Application of Remanent Magnetisation and Self-Demagnetisation Estimation to Mineral Exploration. Extended Abstracts, from the 2013 ASEG-PESA Forum, 41-46.

Pratt, D. A., McKenzie, K. B., and White, A. S., 2012, The remote determination of magnetic remanence: ASEG-PESA 22nd International Geophysical Conference and Exhibition, Extended Abstracts, 5 pp.

Pratt, D.A. 2013, The potential of remote remanence estimation (RRE) for kimberlite exploration – A case history from the Thomson Fold Belt, in P.W. Schmidt, D.A. Pratt, C.A. Foss, eds., The Application of Remanent Magnetisation and Self-Demagnetisation Estimation to Mineral Exploration. Extended Abstracts, from the 2013 ASEG-PESA Forum, 48-54.

Pratt, D.A., McKenzie, K.B. and White, A.S., 2014, Remote remanence estimation (RRE): Exploration Geophysics, **45**, 314-323.

Schmidt, P.W., Pratt, D.A. and Foss, C.A., The Application of Remanent Magnetisation and Self- Demagnetisation Estimation to Mineral Exploration. Extended Abstracts, from the 2013 ASEG-PESA Forum, 79pp.

Schmidt, P.W., and Clark, D.A., 1998, The calculation of magnetic components and moments from TMI: A case study from the Tuckers igneous complex: Exploration Geophysics, 29, 609-614.